Diagnosis of the MJO in an Aquaplanet General Circulation Model

Eric D. Maloney[1], Adam H. Sobel[2], Walter M. Hannah[1]
[1]Department of Atmospheric Science, Colorado State University
[2] Department of Applied Physics and Applied Mathematics, Department of Earth and Environmental Sciences, Columbia University

Correspondence: emaloney@atmos.colostate.edu

1. Introduction

- An MJO in an aquaplanet GCM simulation is analyzed that shows some characteristics of a moisture mode
- The model MJO is destabilized by wind-evaporation feedback, and zonal moisture advection appears to contribute to eastward propagation

2. Model Description

- NCAR Community Atmosphere Model 3
- Swapped in a replacement parameterization for deep convection (we use relaxed Arakawa-Schubert, Moorthi and Suarez 1992).
- T42 horizontal resolution (2.8º x 2.8º), and 26 vertical levels
- Perpetual March 21 insolation and ozone
- Series of 16-year aquaplanet simulations with idealized SST boundary condition containing zonal asymmetries and reduced meridional SST gradient (see **Figure 1** below)

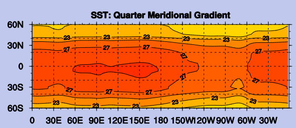

Figure 1. SST distribution for the primary aquaplanet experiment analyzed

3. Eastward Propagation in Unfiltered Fields and Spectra

- Even in unfiltered data, many salient features of the MJO apparent, including 5 m s^{-1} eastward propagation, and a period of 40-60 days (**Fig 2**).
- A strong spectral peak exists at same zonal wavenumber and frequency as observed (**Fig 3**).

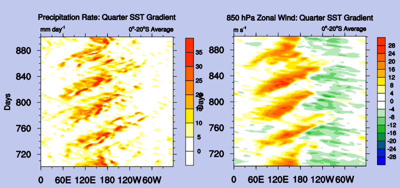

Figure 2. Time-longitude diagrams of 0ºS-20ºS averaged precipitation (mm day^{-1}) and 850 hPa zonal wind (m s^{-1}) for Days 700-900 of the simulation

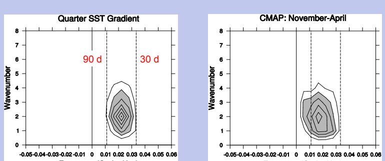

Figure 3. Wavenumber-frequency spectra of equatorial (15ºS-15ºN averaged) precipitation during November-April from CMAP (November-April, right) and the simulation. Contour interval is 0.02 $mm^2\ day^{-2}$, starting at 0.04 $m^2\ s^{-2}$. Values greater than 0.06 $m^2\ s^{-2}$ are shaded.

4. Precipitation Versus Saturation Fraction

- Precipitation is an increasing and strongly non-linear function of saturation fraction of the troposphere (**Figure 4**).

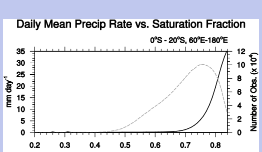

Figure 4. Average daily-mean precipitation rate (solid, mm day^{-1}) versus column saturation fraction in the simulation. Precipitation rate is averaged within saturation fraction bins of width 0.01. The number of observations per bin (gray-dashed) is also shown.

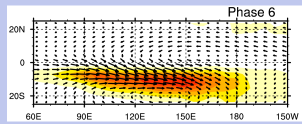

Figure 5. Unfiltered composite 850hPa wind (m s^{-1}) and precipitation (mm day^{-1}) as a function of MJO phase in the simulation. The maximum wind vectors are about 20 m s^{-1}. Maximum precipitation exceeds 28 mm day^{-1}.

5. Composites

- Composites are generated using a similar method to Wheeler and Hendon (2004)
- Unfiltered composites indicate the presence of a westerly jet that lags precipitation by about 5 days (**Figure 5**).
- Precipitation and precipitable water anomalies are nearly exactly in phase (**Figure 6**), as would be expected given the strong relationship between saturation fraction and precipitation

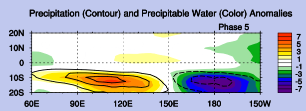

Figure 6. Composite 20-100 day bandpass filtered precipitation and column-integrated precipitable water (mm) anomalies for MJO phase 5 in the simulation. The precipitation contour interval is 4 mm day^{-1}, starting at 2 mm day^{-1}. Negative contours are dashed.

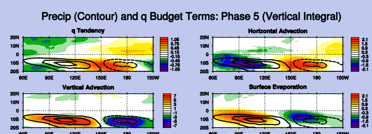

Figure 7. Composite 20-100 day bandpass filtered precipitation anomalies and anomalous column-integrated precipitable water budget terms for MJO phase 5 in the simulation. Terms include column-integrated a) precipitable water tendency, b) horizontal q advection, c) vertical q advection, and d) surface evaporation. Water budget units are mm day^{-1}. The precipitation contour interval is 4 mm day^{-1}, starting at 2 mm day^{-1}. Negative contours are dashed.

6. Moisture Budget

- The vertically-integrated moisture budget is formulated as follows:

$$\left\langle \frac{\partial q}{\partial t} \right\rangle = -\langle q \nabla \cdot \vec{v} \rangle - \langle \vec{v} \cdot \nabla q \rangle + E - P$$

- **Figure 7** shows intraseasonal moisture budget anomalies.
- Horizontal advection is (nearly) in quadrature with precipitation (and PW) and in phase with the humidity tendency.
- Surface evaporation slightly lags the precipitation anomalies, with a strong positive covariance
- Horizontal advection is then partitioned such that overbars represent the 50-day mean and primes the deviations from the 50-day mean:

$$\left(-u\frac{\partial q}{\partial x}\right)' \approx -\bar{u}\frac{\partial q'}{\partial x} - u'\frac{\partial \bar{q}}{\partial x} - \left(u'\frac{\partial q'}{\partial x}\right)'$$

$$\left(-v\frac{\partial q}{\partial y}\right)' \approx -\bar{v}\frac{\partial q'}{\partial y} - v'\frac{\partial \bar{q}}{\partial y} - \left(v'\frac{\partial q'}{\partial y}\right)'$$

- Advection of anomalous humidity by the total zonal wind appears to be essential for eastward propagation (**Figure 8**).

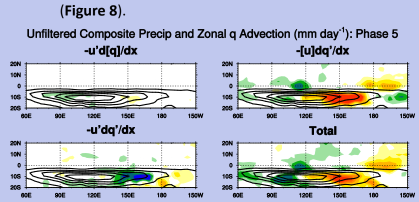

Figure 8. Composite unfiltered partitioned vertically-integrated zonal q advection anomalies (mm day^{-1}) for MJO phase 5 in the simulation. Brackets represent the 50-day mean, and primes deviations from this 50 day running mean. The precipitation contour interval is 4 mm day^{-1}, starting at 0 mm day^{-1}. Tendency is in units of mm day^{-1}.

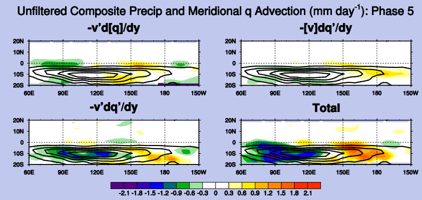

Figure 9. Same as Figure 8, except for meridional advection

7. Sensitivity Tests

A. Remove wind-evaporation feedback by setting surface fluxes to climatology (wind driven component dominates flux)
- WISHE destabilizes the MJO in the model. 30-90 day, wavenumber 1-3 variance decreases dramatically without WISHE active (**Fig 10**)
- Small spatial scale precipitation variability that moves slowly east is still apparent in the model

B. Use SST distribution with reduced zonal gradient (by ½) to test influence of reduced zonal advection through reduction in mean zonal wind
- Propagation speed slowed from 4-5 m s^{-1} to about 2.5 m s^{-1} in the simulation with reduced zonal gradient and reduced westerlies (**Figure 11**).

C. Zonally symmetric SST distribution taken from a Figure 1 north-south cross section at 150ºE.
- Mean easterlies occur everywhere, altering phase relationship between fluxes and precip, and model MJO collapses (**Figure 12**)

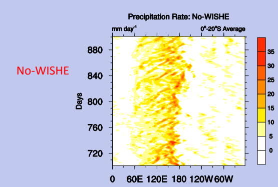

Figure 10. Time-longitude diagrams of 0ºS-20ºS averaged precipitation (mm day^{-1}) and 850 hPa zonal wind (m s^{-1}) for Days 700-900 of the No-WISHE simulation.

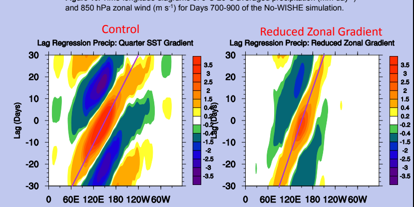

Figure 11. Lag regression of 0ºS-20ºS averaged intraseasonal (20-100 day) precipitation (colors) onto a reference 850 hPa zonal wind time series at 141ºE in a) the control and b) reduced zonal SST gradient simulations. Regression coefficients are scaled by a one standard deviation value of the reference time series. Precipitation anomaly units are mm day^{-1}.

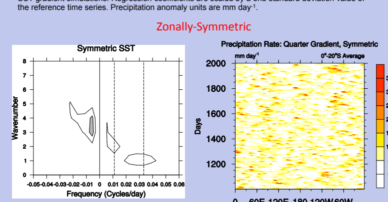

Figure 12. As in Figures 2 and 3, but for the zonally-symmetric case

8. Conclusions

- An MJO in an aquaplanet GCM simulation is analyzed that shows some characteristics of a moisture mode
- The model MJO is destabilized by wind-evaporation feedback, and appears to propagate eastward through advection of anomalous humidity by the sum of perturbation winds and mean westerly flow
- A zonally-symmetric aquaplanet does not support a robust MJO

Acknowledgements: This work was supported by the Climate and Large-Scale Dynamics Program of the NSF under Grant ATM-0632341, under CMMAP cooperative agreement ATM-0832868, and by award NA08OAR4320893 from NOAA. The statements, findings, conclusions, and recommendations do not necessarily reflect the views of NSF, NOAA, or Department of Commerce.